Received 9 September 2023; revised 25 January 2024; accepted 8 February 2024. Date of publication 16 February 2024; date of current version 15 April 2024. The review of this article was arranged by Associate Editor F. Briz.

Digital Object Identifier 10.1109/OJIA.2024.3366524

Experimental Validation of Innovative Control Concepts for Powertrain Test Beds in Power Hardware-in-the-Loop Configuration

DENNIS ERDOGAN [1], ZHANG PENG DU [2], STEFAN JAKUBEK[2], FRANZ HOLZINGER[3], CHRISTIAN MAYR [3], AND CHRISTOPH HAMETNER [1]

[1]Christian Doppler Laboratory for Innovative Control and Monitoring of Automotive Powertrain Systems, TU Wien, A-1060 Vienna, Austria
[2]Institute of Mechanics and Mechatronics, TU Wien, A-1060 Vienna, Austria
[3]AVL List GmbH, A-8020 Graz, Austria

CORRESPONDING AUTHOR: DENNIS ERDOGAN (e-mail: dennis.erdogan@tuwien.ac.at)

This work was supported in part by the Austrian Federal Ministry for Digital and Economic Affairs, in part by the National Foundation for Research, Technology, and Development, and in part by Christian Doppler Research Association.

ABSTRACT Power hardware-in-the-loop (PHIL) testing has become indispensable for the rapid, modular, and cost-saving development of automotive components. This article focuses on PHIL tests composed of entire powertrains that exchange speed and torque signals with vehicle simulations. Previous studies pointed out the importance of promptly following the references from the virtual simulation environment to replicate realistic driving conditions and introduced control strategies to cope with the challenges associated with this setup. However, a comprehensive comparison of the different control strategies has not yet been carried out. To fill this gap, the concepts are first investigated in-depth in simulations and are then, rigorously validated on a state-of-the-art powertrain test bed under highly dynamic driving scenarios, including full-braking. Furthermore, an improvement of existing shaft torque control approaches, which are mainly based on feedforward control, is proposed to better compete with the other methods. The proposed extension shows higher resilience to low accuracy of torque actuators, while the other concepts exhibit greater robustness against time delays. The results from the direct comparisons are summarized and allow the appropriate selection of control strategies for specific use cases.

INDEX TERMS Power hardware-in-the-loop (PHIL), powertrain test bed, speed control, torque control.

I. INTRODUCTION

Hardware-in-the-loop (HIL) trials allow testing of incomplete hardware together with their missing components being simulated. Measurements are sent to the simulation, where the behavior of the nonexisting parts is computed based on a mathematical model [1]. The simulation delivers signals to the hardware, which, depending on the specific test case, are either directly fed to the hardware via actuators or need to be tracked with a controller; see Fig. 1. In order to achieve realistic results, tracking the simulated reference signals as fast as possible is essential. The term power hardware-in-the-loop (PHIL) is used for HIL testing where high power flows between the real component and the simulation are involved [2]. Some publications use the term vehicle-in-the-loop.

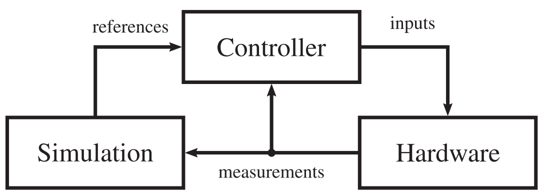

FIGURE 1. **Sketch of a general HIL setup. It is important to track the signals from the simulation fast in order to obtain results that correspond to the reality.**

The focus of this article is the control of entire vehicle powertrain test beds in PHIL configuration, such as the one depicted in Fig. 2. Testing a powertrain in a vehicle exclusively on actual roads is cumbersome and expensive. Well

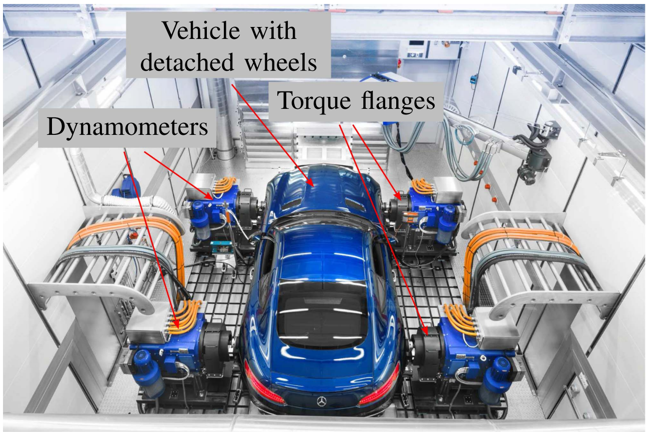

FIGURE 2. Typical structure of a powertrain test bed for PHIL testing with a fully operational vehicle [9].

configured test beds hereby deliver fast and reliable results. For PHIL tests of an entire powertrain, a complete vehicle with detached wheels or the whole powertrain of a vehicle is mounted at the test bed. The wheels are replaced by dynamometers and are simulated together with the road, chassis, and driver. PHIL tests offer a number of advantages. The environmental conditions can be repeated exactly, which cannot be guaranteed for real drives. For example, wet roads or certain road temperatures are simply set in simulation, resulting in independence from the weather. The tests thereby become more reproducible [3]. Especially, for experiments with vehicle dynamic control systems, such as traction control or antilock braking systems (ABS), this is a significant advantage. The effects of small adjustments in these control strategies can be distinguished more easily from random incidents on actual roads and thereby help improve to deliver more fine-tuned vehicle dynamic control systems [4], [5].

Another vast advantage is the parallel design and validation of vehicle components, decreasing development time [6], [7], [8]. For example, a gearbox can be tested without the necessity of a combustion engine or the rest of the drive train. Particularly, the increasingly complex vehicles nowadays contain more and more parts that depend on each other. With PHIL testing, the single components can be tested separately while the missing parts of the vehicle are simply substituted in simulation.

Control algorithms in HIL tests must ensure that signals from the simulation, which serve as reference values, are tracked fast and accurately at the test bed. Otherwise, errors occur that accumulate due to the continuous signal exchange. If, for example, a simulated speed cannot be tracked fast enough at an engine test bed, it also influences the resulting shaft torque, which is fed back to the simulation leading to a vicious circle and overall bad results that do not match the behavior on the road.

Test beds are an integral part of the design and validation of vehicles. They can be employed for technically simple tests, such as torque and power measurements or real driving emissions [10], [11], [12]. With the growing computational power of the recent decades, more and more real driving tests were shifted to virtual testing, where single components could be tested in a PHIL configuration [13], [14], [15], [16]. In the last two decades, the rather simplistic PHIL tests, where the simulation only included driving resistances and road gradients, evolved to highly sophisticated experiments, where test beds are coupled with simulation environments that were initially meant for pure simulation purposes [17], [18]. These types of PHIL tests are the focus in this article. The choice of signals exchanged between the test bed and the simulation (speed- or torque-based control) plays an important role in the performance of the PHIL test and how well the results match real drives.

In [19], the measured speeds at the test bed are fed into the simulation, which on the other hand, returns a torque signal that is applied on the test bed (referred as torque-based approach in this article). However, a feedback controller is not involved in this approach making it vulnerable to uncertainties and inaccuracies at the powertrain test bed, which is one aspect that is tackled in this article.

In contrast, the measured torques at the test bed are sent to the simulation, and the simulated wheel speeds are used as reference signals (referred as speed-based approaches in this article) in [20], [21], [22], and [23]. A slight variation of these speed-based approaches is described in [24], where the knowledge of the closed-loop speed controllers is exploited to modify the reference speed so that the virtual wheel speed can be tracked faster.

In the future, the importance of powertrain testing will even further increase and consequently the control strategies of such systems. Recently, the new topic of connected test beds has arisen, where several spatially distributed components and simulations are connected [25], [26], [27], [28]. Especially, the robustness and reliability of the utilized controllers are crucial, and new challenges are thereby introduced such as higher time delays and jitter.

This article addresses control concepts for powertrain test beds in PHIL configurations, with the focus on obtaining realistic test results. So far, some promising methods have been presented in the literature, but their advantages and disadvantages between each other have not been covered yet. One of the goals of this article is to provide an answer to this. Therefore, three concepts from the literature are thoroughly investigated first in simulation, where the results of a pure vehicle simulation serve as the benchmark for the outcomes of the simulated PHIL test beds. The control concepts are compared with typical shortcomings at powertrain test beds, such as signal noise, incorrectly delivered dynamometer torques, and time delays. Thereby, critical limitations of the different approaches can be explored without endangering the hardware by, for example, potentially harmful instabilities.

Particularly, the torque-based control strategy from [19] seemed appealing due to certain types of interfaces with a restrictive signal exchange between the hardware and the software and because it does not rely on simulated wheel inertia, as later shown. Since a pure feedforward control was used in [19], it lacked the ability to adjust to uncertainties and consequently had a poorer performance compared to the other approaches. Hence, an extension that uses feedback control with a specific reference signal is proposed. In contrast to pure feedforward-based control schemes, where the torques from the simulation are directly used as target values for the dynamometers, this method can compensate for deviations of the desired shaft torques, thereby, improving the performance and accuracy of the PHIL test. The proposed concept proves advantageous, particularly for test beds with dynamometers that provide requested torques imprecisely, i.e., the required torques are only delivered with a gain or offset. The practical feasibility is then validated on a modern powertrain test bed. Before conducting experiments, a system identification is performed to determine parameters that are necessary for the control algorithms. The test runs shown in this publication are highly dynamic maneuvers such as tip-ins and full-braking using an antilock braking system. At the end of this article, a list of advantages and disadvantages of the different concepts shall help choose the most appropriate solution for a certain application. To sum up, the research questions addressed in this publication are as follows.

1) Do the concepts presented for vehicle powertrain PHIL testing in the previous literature deliver the same results in simulation and actual test beds?
2) What are the advantages and disadvantages of those concepts? Under which circumstances is a certain approach favorable compared to the others?

And the highlights are as follows.

1) The proposal of an alternative concept for vehicle powertrain PHIL tests that is torque-based and uses feedback control.
2) Implementation of three control concepts on an actual, modern powertrain test bed in PHIL configuration to prove the technical realization.
3) Direct comparisons on identical test runs using highly dynamic maneuvers that also include the interaction with vehicle dynamics control systems.
4) A thorough analysis of the strengths and weaknesses of each control concept.

The rest of this article is organized as follows. A general overview of a powertrain test bed in PHIL configuration is given in Section II. The differences between dynamometer types and their impact on powertrain PHIL tests are also explained there. In addition, a simple model for the investigations in simulation and the models necessary for the control strategies are introduced. In Section III, the approaches for test bed control alongside the newly developed control concept are presented. Section IV is divided into two major parts. In the first part, the functionality of all methods is checked in simulation under ideal conditions. Also the effects of various uncertainties are analyzed without the risk of harming the actual hardware, and suggestions are given on when to use which method. In the second part, the technical implementation of all control strategies is demonstrated and discussed. Finally, Section V concludes this article.

II. TEST BED SETUP AND MODELING

This section describes the typical structure of a powertrain test bed for PHIL applications and the connection between the simulation and reality. Furthermore, models for both the powertrain test bed and the vehicle simulation with typical modeling assumptions are presented on which the controllers and simulations of the following sections are based. The relevant signals for such applications are also described.

For powertrain testing, a fully operative vehicle is typically utilized, where the wheels are removed and replaced by dynamometers. However, tests with only the powertrain and without the chassis are also possible. Within their connection, torque flanges are used to measure the shaft torque and speed; see Fig. 2. Usually, asynchronous machines (ASM) or permanent magnet synchronous machines (PMSM) are used as dynamometers. Compared to PMSMs, ASMs are less expensive with the drawback of less accurate torque control. Furthermore, the inertia of ASMs is higher, whereas the inertia of PMSMs is more comparable to that of a wheel, which facilitates the control schemes of PHIL tests. However, the higher inertias can also be handled by certain approaches explained in the latter sections. In both cases, the torque is controlled indirectly by measuring the electrical current, which is another uncertainty that needs to be considered.

The missing parts of the vehicle for PHIL testing, i.e., the wheels and the road, are replaced in the virtual simulation environment (VSE); see Fig. 3. The VSE is usually an ordinary vehicle simulation software where the parts that exist in reality are disabled in the software application. In principle, there is either the possibility of sending the measured shaft torque T_{Shaft} at the test bed to the VSE and receiving a virtual wheel speed ω_W that serves as a reference at the test bed or vice versa—sending the measured dynamometer speed ω_D and receiving a virtual shaft torque $T_{\text{Shaft}}^{\text{ref}}$ as a reference. The controller for these virtual signals has to be fast. Otherwise, errors accumulate, or even the whole test can become unstable.

It is also possible to deploy a configuration in which only torque signals or only speed signals are exchanged. However, a feedback controller cannot be applied in this case since this would practically mean that the measured signal is fed into the simulation and then, used as a reference variable for exactly this signal. For example, if the dynamometer speed ω_D is measured and sent to the simulation as an input, it would serve as the virtual wheel speed ω_W there. Consequently, this virtual wheel speed would then be the reference speed for the test bed, which is not reasonable as it is effectively the original measured dynamometer speed. However, it is still possible to carry out PHIL tests in these cases but without using feedback. In the example described above, a simulated resistance torque, such as the tire torque T_{Tire}, can be still directly used for setting the dynamometer torque T_D. In doing

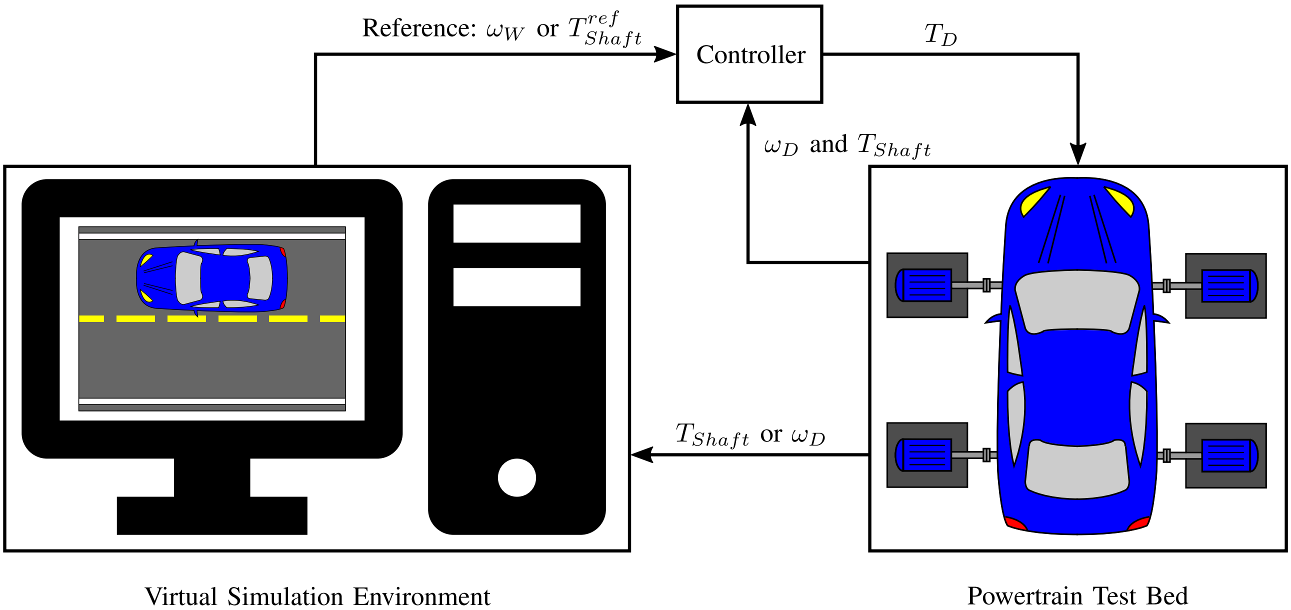

FIGURE 3. PHIL test setup. The coupling from the VSE to the test bed is achieved by the controller, on which it strongly depends whether the tests correspond well to reality.

so, the accuracy of such a test solely relies on the precision of the dynamometers as possible errors cannot be corrected anymore.

A. POWERTRAIN, VEHICLE, AND TEST BED MODELING

For the simulation study, a vehicle model with a simplified powertrain is used, which is based on [29]. To further simplify the simulation model, the vehicle is treated as if there were only one wheel (quarter model), which has little influence on the validity of the simulation results since the measured shaft torques already contain divisive influences on the overall system.

It is noted that the complexity of the vehicle simulation used for PHIL testing can massively vary. In some applications, simple vehicle models that are hardly more sophisticated than the model presented in this section, which may already be adequate for some use cases. For other applications, if the computational power is sufficient, simulation programs originally intended for stand-alone use are utilized.

The engine torque T_E is modeled using a lookup table depending on the throttle position α and the engine speed ω_E, which represents the static behavior of the engine. A first-order differential equation describes the dynamic torque build-up of the engine as follows:

$$\dot{T}_E = \frac{1}{\tau_E}\left(T_{E,\mathrm{LUT}}\left(\alpha, \omega_E\right) - T_E\right) \tag{1}$$

with τ_E denoting the time constant that determines how fast T_E is changing and $T_{E,\mathrm{LUT}}$ the engine torque according to the lookup table. For the investigations in simulation, τ_E has a value of 100 ms, which essentially means that an engine torque step from zero would reach 90% of its target value in around 300 ms (three times τ_E). The connection from the engine to the wheel is modeled as a two-mass oscillator

$$J_E\dot{\omega}_E = T_E - \frac{1}{i}T_{\mathrm{Shaft}} \tag{2}$$

$$J_W\dot{\omega}_W = T_{\mathrm{Shaft}} - T_{\mathrm{Tire}} \tag{3}$$

with J representing the mass moments of inertia, T_{Shaft} the shaft, and T_{Tire} the tire torque. The subscripts E and W denote quantities of the engine and the wheel, respectively. The gear ratio of the transmission is denoted by i.

The shaft torque is modeled as a linear spring-damper system as follows:

$$T_{\mathrm{Shaft}} = k\left(\frac{1}{i}\varphi_E - \varphi_W\right) + c\left(\frac{1}{i}\omega_E - \omega_W\right) \tag{4}$$

with φ denoting the angular positions, ω the angular velocities, k is the stiffness, and c the damping coefficient of the powertrain.

Although, the powertrain and especially the gearbox is simplified through this model, it does not play a significant role in investigating different PHIL testing strategies. The tire force is computed by

$$F_{\mathrm{Tire}} = C_L\lambda \tag{5}$$

where C_L is the longitudinal tire stiffness, and λ is the slip which is defined as

$$\lambda = \frac{\omega_W r - v}{\omega_W r} \tag{6}$$

with r as the tire radius and v the vehicle speed. Subsequently, the tire torque can be calculated as $T_{\mathrm{Tire}} = F_{\mathrm{Tire}}r$. The vehicle itself is modeled as a point mass. Using the principle of linear

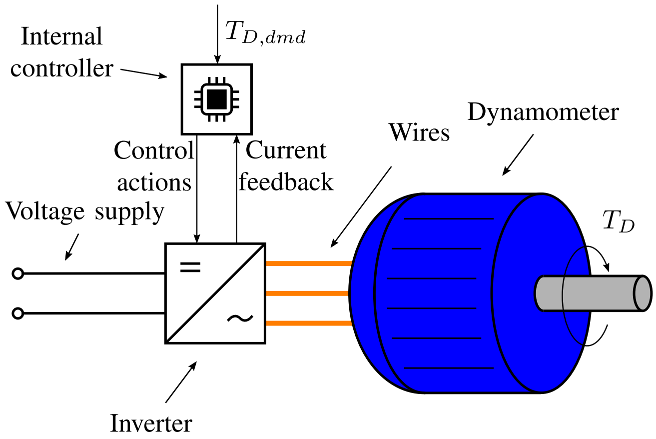

FIGURE 4. Schematic of a dynamometer and the electric drive with its internal controller.

momentum, the following equation is derived:

$$m\dot{v} = F_{\text{Tire}} - av^2 - bv - c\,\text{sign}(v) \tag{7}$$

where m denotes the mass of the vehicle and a, b, and c friction coefficients.

With (1)–(7), the simple vehicle model is complete. By solely looking at (3), one might think that the overall vehicle inertia m does not play a role in the simulation. However, the tire torque indirectly accounts for the vehicle mass as it depends on the tire slip, which, on the other hand, is a result of the vehicle speed in (7). It is also noted that there is almost always a certain tire slip, even when the whole system runs in steady-state at a constant speed due to the friction in (7).

At the test bed, dynamometers are attached instead of the wheels. In Fig. 4, a dynamometer, an inverter, and its internal controller are depicted. Strictly speaking, a dynamometer is a device that simultaneously measures torque and angular velocity. In the context of automotive test beds, dynamometers are usually electrical motors used as loads for the unit under test. The torque is indirectly determined by the measured current of the dynamometer as these two entities almost share a linear relation to each other. Therefore, a demanded torque $T_{D,\text{set}}$ is turned into a current demand first. The internal controller drives the inverter and modulates the voltages between the phases of the electric motor in such a way that this demanded current and, consequently, the demanded torque is reached. This inner control loop runs on a separate device with lower sampling times and can reach the target torque so fast that the following assumption can be made:

$$T_{D,\text{set}} = T_D. \tag{8}$$

For further details on the control of electrical machines, the reader is referred to, e.g., [30].

For the simulations of the powertrain test bed, (3) is replaced by

$$J_D\dot{\omega}_D = T_{\text{Shaft}} - T_D \tag{9}$$

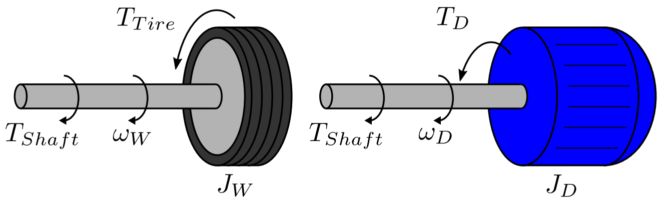

FIGURE 5. Inertia of the simulated wheel (left) and the one with the dynamometer at the test bed (right) differ. However, the similarities of the two systems can be exploited for a feedforward controller by either directly using the simulated tire torque T_{Tire} as the requested dynamometer torque T_D or implementing an inertia compensation by trying to enforce the same angular acceleration on the virtual and actual system.

with the subscript D representing the dynamometer quantities. The shaft torque at the test bed is now defined as

$$T_{\text{Shaft}} = k\left(\frac{1}{i}\varphi_E - \varphi_D\right) + c\left(\frac{1}{i}\omega_E - \omega_D\right). \tag{10}$$

For the simulation of a PHIL test, the powertrain and the vehicle are computed separately and exchange only a few signals that are artificially delayed and contain additional noise and other uncertainties. The effect of the tires is substituted with the dynamometer, which has to emulate the tire behavior and also introduces errors. These deficiencies are part of the examinations in this article.

III. CONTROL METHODS FOR POWERTRAIN PHIL TESTING

In order to perform realistic PHIL testing at powertrain test beds, which correspond to real drives well, proper control strategies need to be chosen that follow the given reference signals from the VSE fast. Here, two advanced strategies from the literature are presented, which are both speed-based controllers. Moreover, a third control method is proposed to fill the gap of a torque-based controller that runs with a feedback control scheme and allows connections to VSEs, which only return torque signals, in a realistic manner. Before the three controllers are described in detail, a feedforward control scheme is shown first, a common part of two of the following concepts. The controllers are each developed for one wheel and work independently of each other.

A. FEEDFORWARD CONTROL FOR INERTIA COMPENSATION

In order to enhance the reference tracking at powertrain test beds, a feedforward control law is used in some of the control schemes presented in the following sections. The goal is to shift the workload of the feedback controller to the feedforward controller, which is beneficial as feedback controllers only start acting when there is already a control error.

Obviously, (3) describing the simulated vehicle and (9) characterizing the test bed are similar. In Fig. 5, the similarities between the simulation and real components at the test bed are visualized, where the left sketch shows the shaft and the wheel, and the right sketch shows the shaft at the test

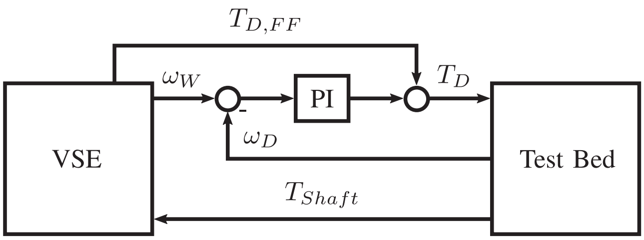

FIGURE 6. **Block diagram of the speed controller with T_{Tire} used as a feedforward control signal. Deviations between the simulated speed and the speed at the test bed are handled by a PI controller.**

bed with the dynamometer. By comparing (3) and (9), a good guess of the feedforward dynamometer torque $T_{D,FF}$ would be therefore

$$T_{D,FF} = T_{\text{Tire}}. \tag{11}$$

The inertia of the dynamometer J_D is usually higher than the inertia of the wheel J_W. Higher mismatches between these values make it advantageous to utilize an inertia compensation. Especially, ASMs usually have considerably heavier inertias than the wheels of a vehicle. The inertia compensation is derived by demanding the angular accelerations of the wheel in simulation and the dynamometer in reality, see (3) and (9), to be equal

$$\dot{\omega}_W \overset{!}{=} \dot{\omega}_D. \tag{12}$$

Substituting (3) and (9) into (12) leads to the feedforward control law

$$T_{D,FF} = \frac{J_D}{J_W} T_{\text{Tire}} + \left(1 - \frac{J_D}{J_W}\right) T_{\text{Shaft}}. \tag{13}$$

As the considered test bed for the experimental validation is equipped with PMSMs, (11) is already sufficient and therefore utilized in the following investigations. Equation (13) is mentioned here only for the sake of completeness. It is also noted that there are possibilities for applying an inertia compensation without using a torque sensor, for example, in [31].

B. SPEED CONTROL IN COMBINATION WITH FEEDFORWARD CONTROL

This controller works with the given speed of the VSE ω_W and tries to follow this signal with the dynamometer speed ω_D at the test bed as accurately as possible [21], [22]. The inputs to the VSE are the measured shaft torques T_{Shaft} that result from the powertrain that drives the whole system and the dynamometers that are used to emulate the tire and the road. In Fig. 6, a block diagram of a PHIL setup with speed control is depicted. As a feedback controller, a simple PI controller with the empirically determined controller parameters K_P and K_I is employed. Ideally, this controller only corrects minor deviations as there is the tire torque T_{Tire} as the feedforward control signal. In summary, the following 2-DOF control law emerges:

$$T_D = -K_P\left(\omega_W - \omega_D\right) - K_I \int_0^t \left(\omega_W - \omega_D\right) d\tau + T_{D,FF} \tag{14}$$

with $T_{D,FF}$ defined in (11). The negative signs in this equation are due to the dynamometer torque being defined as a load. Provided that the simulation represents the actual vehicle well, the PHIL test matches the reality well if the speed deviation at the test bed can be kept low.

C. SPEED CONTROL WITH REFERENCE MODIFICATION

This concept was proposed in [24] and is also based on controlling the speeds of the powertrain test bed and feeding the measured shaft torques to the VSE. In contrast to the previous concept, the key idea is to modify the reference speed ω_{ref} to the PI controller in order to improve the reference tracking leading to more realistic PHIL testing. The PI controller is only tuned roughly as the modified speed for the controller already takes this into account.

The necessary closed-loop transfer function $G_{cl}(s)$, with s denoting the Laplace variable, is derived by first calculating the open-loop system consisting of the PI controller and (9) Laplace transformed, which describes the relevant parts of the test bed for the speed control

$$G_o(s) = \underbrace{\frac{K_P s + K_I}{s}}_{\text{PI controller}} \frac{-1}{J_D s}. \tag{15}$$

Again, the negative sign in this equation is due to the dynamometer torque being defined as a load. The shaft torque T_{Shaft} in (9) is ignored at this point and will be considered later on. With (15), the closed-loop system is calculated

$$\frac{\omega_D(s)}{\omega_{\text{ref}}(s)} = G_{cl}(s) = \frac{G_o(s)}{1 + G_o(s)}. \tag{16}$$

To further increase the dynamics of the test bed, a modified speed ω_{mod} is used instead of the simulated wheel speed ω_W, which would usually be the desired value ω_{ref} at the test bed

$$\omega_D(s) = G_{cl}(s)\omega_{\text{mod}}(s). \tag{17}$$

In order to overcome the closed-loop dynamics of the test bed, the modified speed is defined as

$$\omega_{\text{mod}}(s) = \frac{1}{G_{cl}(s)}\omega_W(s). \tag{18}$$

By the inversion of the closed-loop system, a noncausal control law emerges where the order of the numerator is higher than the order of the denominator by one, making it nonapplicable in an actual controller. The idea to overcome this noncausality is to exploit the integrator in (3), which is already used in the vehicle simulation. In the Laplace domain, (3) is defined as

$$\omega_W(s) = \frac{1}{J_W s}\left(T_{\text{Shaft}}(s) - T_{\text{Tire}}(s)\right). \tag{19}$$

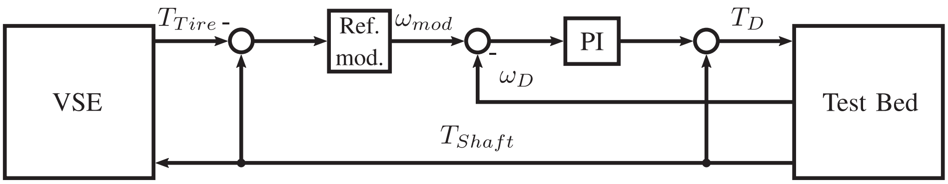

FIGURE 7. **Block diagram of the speed controller with reference modification. The reference speed for the PI controller is manipulated in such a way that it increases the overall reference tracking speed.**

Inserting (19) and (18) into (17) leads to

$$\omega_D(s) = G_{cl}(s) \underbrace{\frac{1}{G_{cl}(s) J_W s} \left(T_{\text{Shaft}}(s) - T_{\text{Tire}}(s)\right)}_{\omega_{\text{mod}}(s)}. \tag{20}$$

As a consequence, the order of the denominator is increased by one leading to a causal and therefore feasible control law. Instead of the simulated wheel speed ω_W, the resulting torque $T_{\text{Shaft}} - T_{\text{Tire}}$ at the wheel is now used. Overall, the following control law emerges:

$$\begin{aligned} T_D = &- K_P \left(\omega_{\text{mod}} - \omega_D\right) \\ &- K_I \int_0^t \left(\omega_{\text{mod}} - \omega_D\right) d\tau + T_{\text{Shaft}} \end{aligned} \tag{21}$$

where the shaft torque T_{Shaft}, which was ignored in the whole derivation, is also added. The complete concept is visualized as a block diagram in Fig. 7. In contrast to the other methods, the formulation in (21) allows an inherent inertia compensation, and (11) is not necessary.

D. TORQUE CONTROL IN COMBINATION WITH FEEDFORWARD CONTROL

The last concept presented here is a torque-based controller with feedback in combination with the feedforward controller. Compared with the previous approaches, the VSE works with the measured speed ω_D of the test bed instead of the shaft torque T_{Shaft} and instead of controlling the speed at the test bed the torque is now controlled. Torque-based controllers have already been employed for powertrain test bed control in PHIL configuration [19]. However, only a feedforward control scheme has been utilized up until now. As a result, these controllers rely on accurate dynamometers as they cannot correct potential deviations leading to results that do not correspond to reality well. Therefore, a feedback loop is intended to remedy the situation. Instead of measuring torque and controlling the speed at the test bed, it is the other way around, which is advantageous for vehicle simulation software that only allows the signal flow in this manner.

Generally, the VSE does not provide a suitable reference signal for the shaft torque because it is not included in the simulation. However, an expected shaft torque $T_{\text{Shaft}}^{\text{ref}}$ can be calculated based on (9)

$$T_{\text{Shaft}}^{\text{ref}} = T_{D,FF} + J_D \dot{\omega}_D. \tag{22}$$

Since the acceleration of the dynamometers cannot be measured directly, it needs to be computed numerically. A convenient solution is to utilize a low-pass filter with a time constant τ

$$T_{\text{Shaft}}^{\text{ref,filt}}(s) = \frac{1}{\tau s + 1} T_{D,FF}(s) + \frac{J_D s}{\tau s + 1} \omega_D(s). \tag{23}$$

The time constant was set to 0.001 s, which is quite fast in order to prevent high phase lags and still get rid of noise in the differentiated speed.

Again, an empirically tuned PI controller is utilized in this control scheme. With (23) and (11), the control law results to

$$\begin{aligned} T_D = &K_P \left(T_{\text{Shaft}}^{\text{ref,filt}} - T_{\text{Shaft}}^{\text{filt}}\right) \\ &+ K_I \int_0^t \left(T_{\text{Shaft}}^{\text{ref,filt}} - T_{\text{Shaft}}^{\text{filt}}\right) d\tau + T_{D,FF} \end{aligned} \tag{24}$$

with T^{filt} as a filtered version of the shaft torque T_{Shaft} using the same low-pass filter as in (23). A block diagram of the whole concept is depicted in Fig. 8. Without the PI controller, this method would be identical to [19], which does not take actions in case the actual load is not reached due to disturbances and uncertainties.

IV. RESULTS

The three described controllers of the last section for powertrain testing in PHIL configuration are compared in this section. First, investigations in simulations are shown, where PHIL tests are conducted on typical vehicle maneuvers to examine the differences in performance under different circumstances between the methods. These investigations can be carried out in simulation without the risk of harming the actual hardware. The robustness of the control concepts is tested against a variety of typical uncertainties and deficits that occur at test beds, such as measurement noise, time delays in communication, and wrongly delivered dynamometer torques. These simulation results show the advantages and disadvantages of the controllers under different situations and shall help decide which method to utilize for known shortcomings at specific test beds. In order to prove the technical realization of all presented concepts, they are implemented on an actual, modern powertrain test bed similar to the one shown in Fig. 2. The different methods are compared on highly dynamic maneuvers, including tip-ins/tip-outs and full-braking tests. Due to confidentiality agreements, a comparison with real-world driving data cannot be shown.

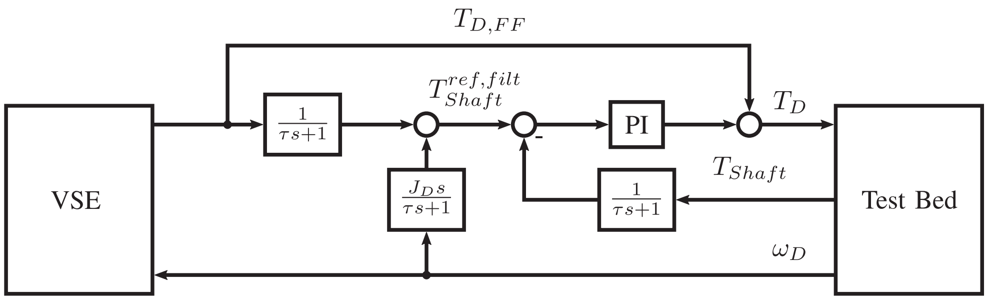

FIGURE 8. Block diagram of the torque controller with feedforward control. An expected shaft torque $T_{\mathrm{Shaft}}^{\mathrm{ref,filt}}$ at the test bed is calculated and controlled by a PI controller. The low-pass filters are necessary in order to compute the derivative of the test bed speed.

For the simulation, the quarter model derived in Section II is utilized, and consequently, only one controller is required. At the real test bed, on the other hand, each vehicle wheel is replaced by a dynamometer, and a controller runs on each of them separately and independently.

A. CONTROLLER VALIDATION AND COMPARISON IN SIMULATION

The simulation results in this section shall give an idea of how each control concept for powertrain PHIL tests performs with the presence of uncertainties to choose the optimal controller for specific circumstances at the test bed. Simulations are performed for which the MATLAB/Simulink environment was chosen to avoid the risk of damage to the expensive test bed hardware. All tests are first conducted with a pure vehicle simulation that uses (1)–(7) to describe the entire vehicle and serves as the benchmark. For the simulation of the PHIL tests, (1), (9), and (10) are used for the simulated test bed, and (3)–(7) are used for the simulated VSE. The interactions of the wheels through the differential gears do not need to be considered as possible interactions can be immediately observed via the torque measurement and controlled independently. Not only were the simulations utilized for examinations, but they were also used for a rough tuning of the controller parameters offline.

The following are typical uncertainties that occur at powertrain test beds and potentially lead to distorted and unrealistic test results:

1) measurement noise;
2) time delays in the communication; and
3) inaccuracies in the dynamometer torques.

In both the VSE and the control loop, noise can lead to oscillations and thus, compromise the outcome of PHIL tests. Between the connection of a test bed and a VSE, time delays occur due to the communication. Typically, bus systems like CAN are used to exchange signals, which only transmit at certain intervals. Furthermore, the time necessary for a simulation step also adds up to the delay. Generally, time delays have a bad impact on the stability of systems and are therefore examined in this article. The dynamometer torques can only be measured indirectly by the current to the electrical motors, which may lead to the dynamometer delivering the wrong torques depending on the operating point. With the shaft torque sensor, the dynamometer torques cannot be determined as they only match in stationary running; see (9). As a consequence, test results might be compromised, especially, if no feedback controller is involved in the control strategy.

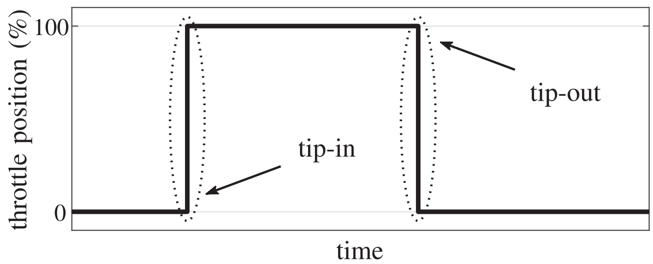

FIGURE 9. Tip-in/tip-out maneuver. The sudden changes in the throttle position cause oscillations in the whole powertrain.

For the investigations in simulation, the so-called tip-in/tip-out maneuver is chosen as a test scenario, which is depicted in Fig. 9. The vehicle coasts down from an initial speed. Since there is no drive, the vehicle slows down due to friction. The throttle is fully actuated after a certain time (tip-in), leading to oscillations in the whole powertrain. After some time, the throttle is fully released (tip-out). This sudden change causes oscillations again. Tip-ins/tip-outs are used in the industry to calibrate comfort functionalities and are generally a benchmark test for PHIL tests.

In Fig. 10, the simulation results under ideal circumstances without any uncertainties are shown. The solid lines represent the results of the pure simulation (benchmark), the dashed lines the speed control with feedforward control (speed control), the dotted line the speed control with reference modification (speed mod.), and the dashed-dotted lines the torque control with feedforward control (torque control). In the upper plot, the longitudinal acceleration is depicted. The virtual wheel speed is displayed for comparison in the diagram below since no dynamometer speed is available in the benchmark simulation. In the case of the torque controller, the virtual speed and the dynamometer speed are equivalent since the measured speed is used in the simulation; see Section III. Until time 0.25 s, the throttle position α is set to zero, and the

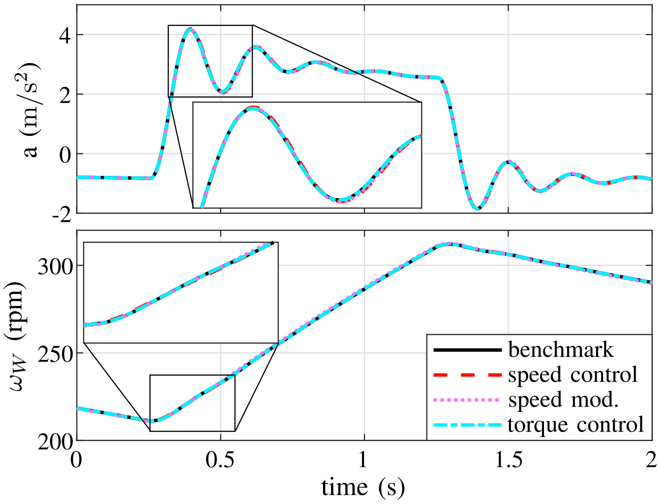

FIGURE 10. Tip-in/tip-out maneuver in simulation under ideal conditions.

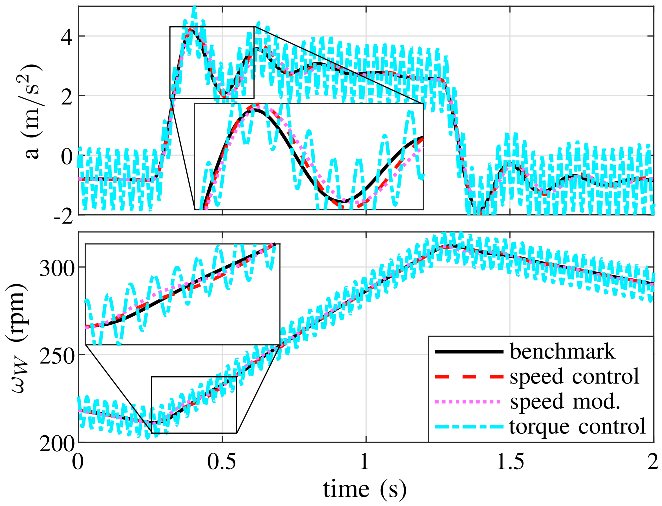

FIGURE 12. Tip-in/tip-out maneuver in simulation with time delays in the communication between test bed and VSE.

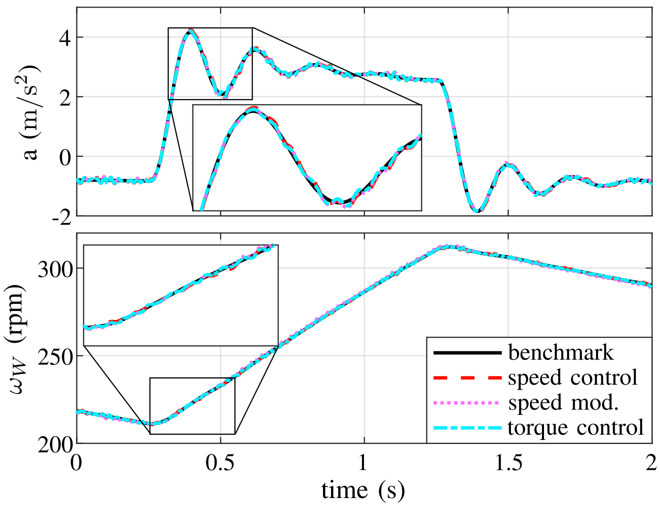

FIGURE 11. Tip-in/tip-out maneuver in simulation with measurement noise.

vehicle coasts. Then, the throttle suddenly increases to 100%, which results in oscillations in the acceleration signal. Simultaneously, the wheel speed also starts to increase. At time 1.25 s, the throttle is fully released ($\alpha = 0$). Consequently, oscillations occur through the strained powertrain, and the vehicle coasts down again.

As visualized in Fig. 10, all three control strategies lead to satisfying results close to the benchmark's findings. The performance of the controllers and their behavior against uncertainties strongly depend on their tuning. Therefore, the controllers were tuned to deliver similar results under ideal conditions to ensure a fair comparison.

In Fig. 11, the first investigation is shown where the effect of measurement noise is examined. The noise is added to the measured dynamometer speed and the shaft torque with a signal-to-noise-ratio of around 15. Even though the control concepts use different signals for feedback control and interaction with the VSE, their sensitivity to measurement noise is similarly robust. While the noisy shaft torque is sent to the VSE in the case of the speed control with feedforward control, it is utilized for feedback control in the torque control concept. For the speed signal, it is vice versa. Thus, a deficiency in a signal always has an effect no matter what method is used.

In the next test, the robustness against time delays is examined. The results are depicted in Fig. 12, where a time delay of 10 ms in both signal directions is used. While the speed control with feedforward control and the speed control with reference modification both still deliver decent outcomes, the torque controller is far more sensitive to time delays. The reason for this is the wheel slip computation in (6). A small change in the wheel speed has vast effects on the wheel slip λ and consequently on the tire force F_{Tire}. Through the delayed speed signals to the VSE, F_{Tire} largely varies, resulting in a greatly varying simulated torque that corresponds to the demanded torque at the test bed. On the other hand, a delayed shaft torque for both speed control based methods is less critical since the wheel speed is calculated in the VSE via (3) and allows more deviations from the actual signal. Note that the assumed time delays are unrealistically high for investigation examination purposes. Nevertheless, such delays might occur for systems with older hardware or at connected test beds, where the hardware is distributed to different locations; see [25], [26], [27], and [28].

In Fig. 13, the effects of dynamometer wrongly applied torques are investigated. As already mentioned in previous sections, the dynamometer torque is not measured directly but computed via the electrical current in the machine. Especially, electrical machines of type ASM are prone to considerable torque deviations [32]. For a PHIL test at powertrain test beds, the dynamometer torque T_D serves as the control input. If the demanded torque cannot be reached, the feedback controllers

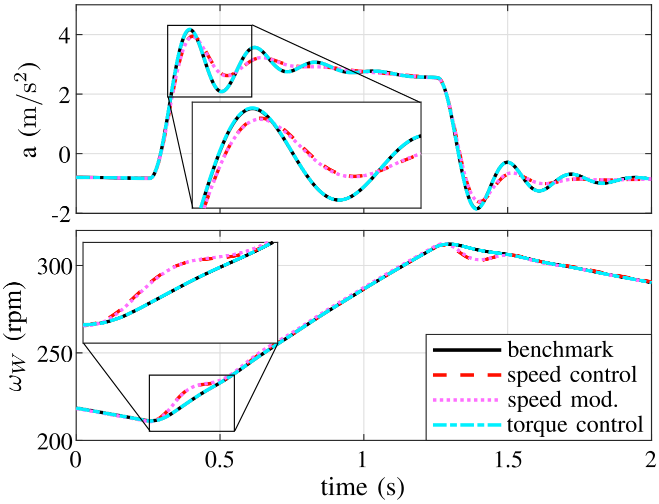

FIGURE 13. Tip-in/tip-out maneuver in simulation with the dynamometer torque multiplied by a factor of 0.85.

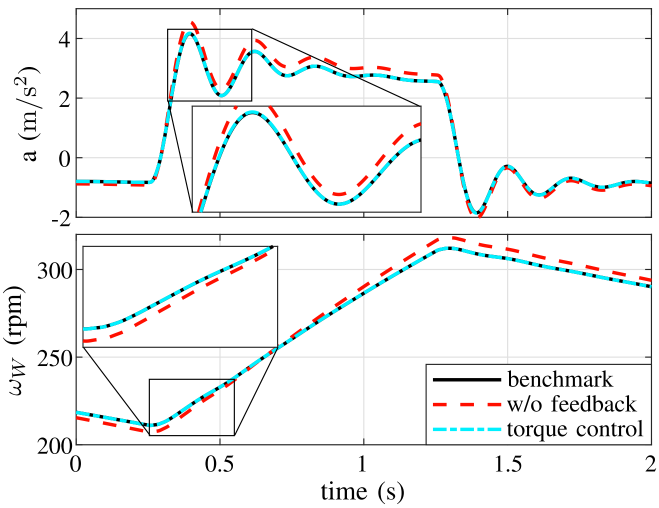

FIGURE 14. Tip-in/tip-out maneuver in simulation with the dynamometer torque multiplied by a factor of 0.85. Here, the red dashed line represents the torque-based method without the use of feedback.

of the control schemes need to correct this inaccuracy. For the investigations, T_D was multiplied by different scaling factors. A factor of 0.85 is used for the results in Fig. 13, which can be considered as a pessimistic assumption for the real world. There, the torque control strategy has an advantage over the control concepts that are based on speed control. Its outcomes follow the benchmark results more closely. As the torque controller has more direct access to the torques in general, it is able to react faster to deviations in these entities and is therefore also quicker in correcting the dynamometer torque. Especially, after the throttle steps, the speed control concepts need some time to adjust the correct torque.

The last examination in simulation is depicted in Fig. 14, where the effect of using a pure feedforward torque control scheme compared to the new torque-based controller is examined (essentially the method proposed in [19]). It underlines the importance of torque feedback and why this method was proposed in the first place. Once again, the dynamometer torque is scaled by a factor of 0.85. This time, the dashed line represents the results of the sole use of the feedforward control scheme; see (11). The dynamometer torque is again lower than both controllers expect. However, while the new torque controller can compensate for the deviation of the requested torque, the pure feedforward controller delivers poor outcomes. In fact, it even starts with a wrong initial speed. While the vehicle is coasting, the simulated vehicle inertia actually propels the test bed. With less torque, the test bed slows down faster. The opposite is the case when the throttle step happens. Now, the vehicle inertia counteracts the acceleration. Again, less torque is applied than the controller anticipates, so the vehicle accelerates faster than the benchmark.

TABLE 1 Advantages and Disadvantages of the Presented Control Concepts Under Different Circumstances

	Speed Control	Speed Mod.	Torque Control
Noisy Measurements	effective	effective	effective
Time Delays	effective	effective	insufficient
Dyno Torque Errors	adequate	adequate	effective

In general, the simulations demonstrate that all control concepts work well. It is also shown that they have different advantages and disadvantages against particular uncertainties. With this knowledge, an appropriate control strategy can hereby be chosen if shortcomings of a powertrain test bed are known. To sum up, the speed control with feedforward control and the speed control with reference modification are especially beneficial for systems with high time delays. Regarding measurement noise, all concepts have shown to be robust with similar performance. On the other hand, the torque control with feedforward control is advantageous for systems where the dynamometer cannot accurately deliver torque. In particular, this concept is interesting for powertrain test beds that are equipped with ASMs. Another benefit of the torque control is that it can be conveniently used at test beds where the VSE only accepts measured wheel speeds and no shaft torques as inputs. The performances of the speed control based approaches are similar, and therefore, the choice is more a matter of personal preferences. The advantages and disadvantages are also concisely shown in Table 1.

B. EXPERIMENTAL VERIFICATION OF THE TECHNICAL FEASIBILITY

The actual, technical realization of all concepts is demonstrated on a state-of-the-art powertrain test bed. An upper-class vehicle with four-wheel drive with about 450 kW power is employed at the test bed. The dynamometers are PMSMs and provide up to 3500 Nm each. AVL VSM is used as the simulation environment, which is designed for pure vehicle simulations; see [9]. The experiments were conducted using a tip-in/tip-out test and, in the end, full-braking maneuver with

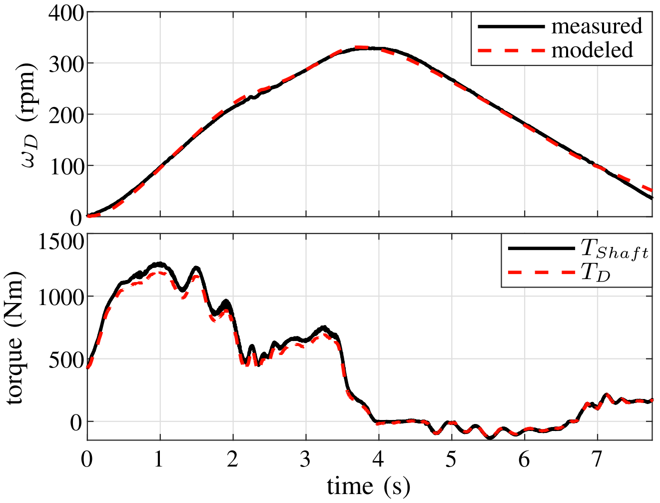

FIGURE 15. Comparison between the measured dynamometer speed and the output of the identified model of the rear left side of the vehicle.

ABS. All comfort functionalities of the vehicle are deactivated while the tests in the following sections are conducted. Due to confidentiality agreements, this article cannot show comparisons with road measurements, but the PHIL test in speed control configuration matched the road measurements and can, therefore, be seen as a benchmark here. Before presenting the results of the maneuvers, a system identification is shown first.

1) PARAMETER IDENTIFICATION OF THE TEST BED

The correct knowledge of the parameters of the powertrain test bed is crucial for the performance of PHIL tests. In order to not rely on potentially inaccurate parameters from data sheets, a short system identification is carried out [33]. Hereby, the goal is to estimate the inertia of the dynamometer in combination with the additional shaft that is not part of the vehicle. A gray box system identification was carried out based on the following differential equation:

$$J_D \dot{\omega}_D = T_{\mathrm{Shaft}} - T_D - c_1 \omega_D - c_2 \qquad (25)$$

where the shaft torque T_{Shaft} is considered the powering torque, the dynamometer torque T_D is the load, c_1 denotes a speed proportional friction coefficient, and c_2 is a static friction. For the evaluation of the parameter estimation, the Matlab System Identification Toolbox was used [34]. The measurement data taken for the identification process are from preliminary test runs where tip-in maneuvers were performed in PHIL configuration. In Fig. 15, the outcome of the parameter estimation is shown. The solid line in the upper plot shows the measured dynamometer speed, whereas the dashed line shows the model output of (25). In the lower diagram, the solid line represents the shaft torque, and the dashed line the dynamometer torque. The resulting torque $T_{\mathrm{Shaft}} - T_D$ accelerates the test bed in the first half of the experiment, while it decelerates by the friction in the second half. As shown, the model can represent the system sufficiently with low deviations.

TABLE 2 Average Estimated Dynamometer Parameters

J_D	c_1	c_2
$3.03\ \mathrm{kg \cdot m^2}$	$0\ \mathrm{Nm \cdot s/rad}$	$25.2\ \mathrm{Nm}$

The estimated parameters of all four dynamometers have a maximum deviation of 15%, and their average values are listed in Table 2. Interestingly, the speed proportional friction coefficient c_1 is zero, which means that the friction is constant and does not depend on the speed. If a larger range of velocities had been covered, it might be possible to detect speed proportional friction. However, the friction is certainly dominated by the static friction. For simplicity, a common inertia instead of individual parameters for each powertrain side is chosen for the control schemes in next sections.

2) TIP-IN/TIP-OUT TESTING

In contrast to the investigations in simulation, the controllers presented are now used on all sides, i.e., four times. The controllers work independently of each other. As the rear axle works with greater power and torques, it was used intentionally, and the rear left side was used randomly to portray the results. The first PHIL test presented is again the tip-in/tip-out maneuver. Here, the throttle position is set from 0% to 100% after a coast-down and released after a certain engine speed is reached, with the process carried out in the same gear. Through the sudden change in the throttle position, the generated engine torque also varies quickly, leading to oscillations in the whole powertrain. This test is dynamically demanding, but it is also a relevant scenario on test beds in which comfort functionalities for vehicles are tuned and where powertrain test beds with their identical conditions and additional sensors are more beneficial than real road tests.

In Fig. 16, the tip-in/tip-out maneuver results are depicted. The dashed line represents the speed control with feedforward control (speed control), the dotted line the speed control with reference modification (speed mod.), and the dashed-dotted line the torque control with feedforward control (torque control). In the upper diagram of Fig. 16, the simulated longitudinal vehicle acceleration a is displayed, while in the diagram below, the dynamometer speed ω_D of the rear left side is depicted. In the beginning, the vehicle is coasting, leading to a slight deceleration until the throttle is fully actuated at around 0.5 s. The sudden change causes the whole powertrain to oscillate, as the measurements in Fig. 16 show. All three control strategies lead to almost the same results. The minor deviations between the runs emerge partly by chance and change from run to run. More significant differences in the performance could not be observed. It is noted that the testing time was somewhat limited and that the results displayed here were generated with the controller parameters that were solely tuned in the simulation, indicating that all concepts are easy to implement in practice.

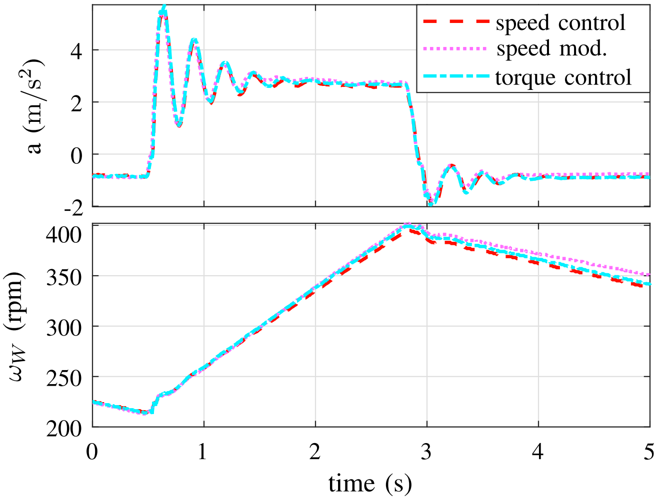

FIGURE 16. Tip-in/tip-out maneuver on the test bed with different methods.

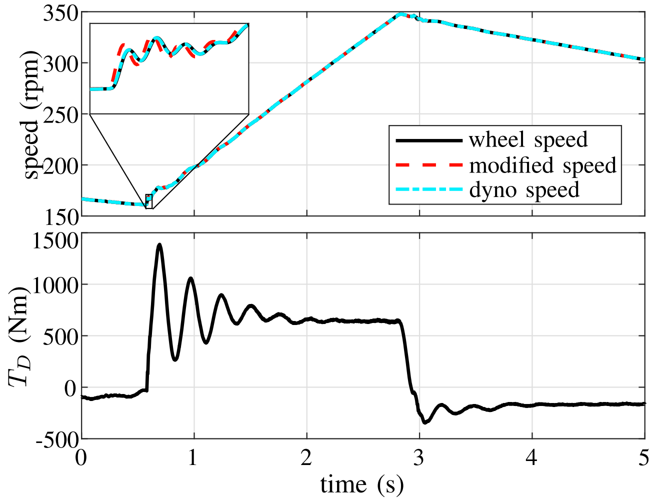

FIGURE 18. Tip-in/tip-out maneuver on the test bed with speed control and reference modification.

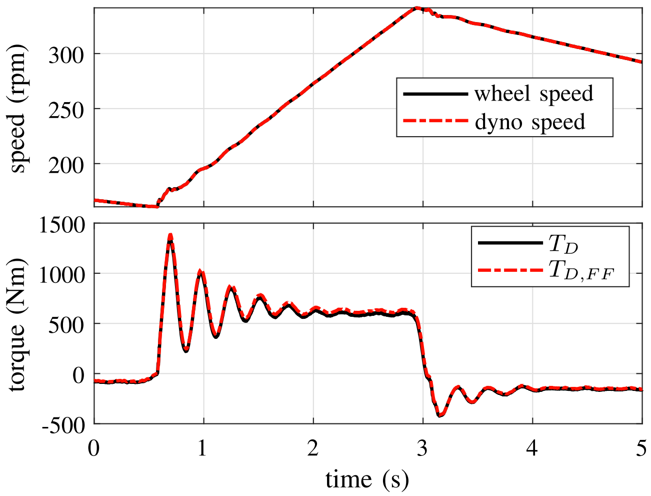

FIGURE 17. Tip-in/tip-out maneuver on the test bed with speed control and feedforward control.

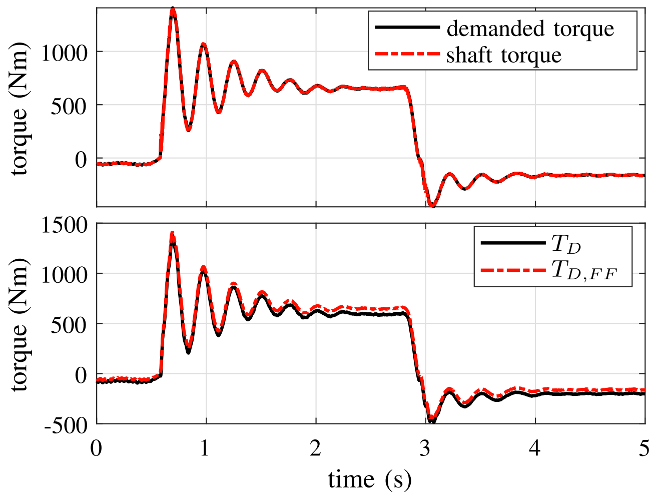

FIGURE 19. Tip-in/tip-out maneuver on the test bed with torque control and feedforward control.

The next figures show the individual concepts in detail. In Fig. 17, the speed control in combination with the feedforward control is visualized. The upper plot shows the rotational speeds of the rear left side of the vehicle, with the solid line representing the simulated wheel speed ω_W, and the dash-dotted line the dynamometer speed ω_D at the test bed. In the diagram below, the input torque is shown, where the dash-dotted line displays the output of the feedforward controller, which is essentially the simulated tire torque T_{Tire}; see Section III. The black line indicates the total torque applied at the test bed. For this concept, the wheel speed ω_W is the reference signal for the controller. The diagram shows that the dynamometer accurately follows the reference. However, this is necessary because minor errors would already sum up to large deviations due to the interaction with the virtual simulation. The feedforward control handles the central part of the input signal. Only a slight correction needs to be performed by the PI controller.

The speed control with reference modification is analyzed in Fig. 18. In the upper diagram, the solid line represents the simulated wheel speed ω_W, which in the end, is the desired value for the dynamometer speed ω_D depicted by the dash-dotted line. The modified speed, which is provided for the PI controller, is depicted by the dashed line. Through the modification, the dynamics of the closed-loop system shall be overcome; see (20). In the lower diagram, the input signal is shown without a feedforward signal since this control strategy does not provide it. The effect of the modified speed can be observed especially at the beginning of the tip-in, where the modified speed overshoots in comparison to the actual desired speed in such a way that the dynamometer speed almost perfectly matches the simulated wheel speed.

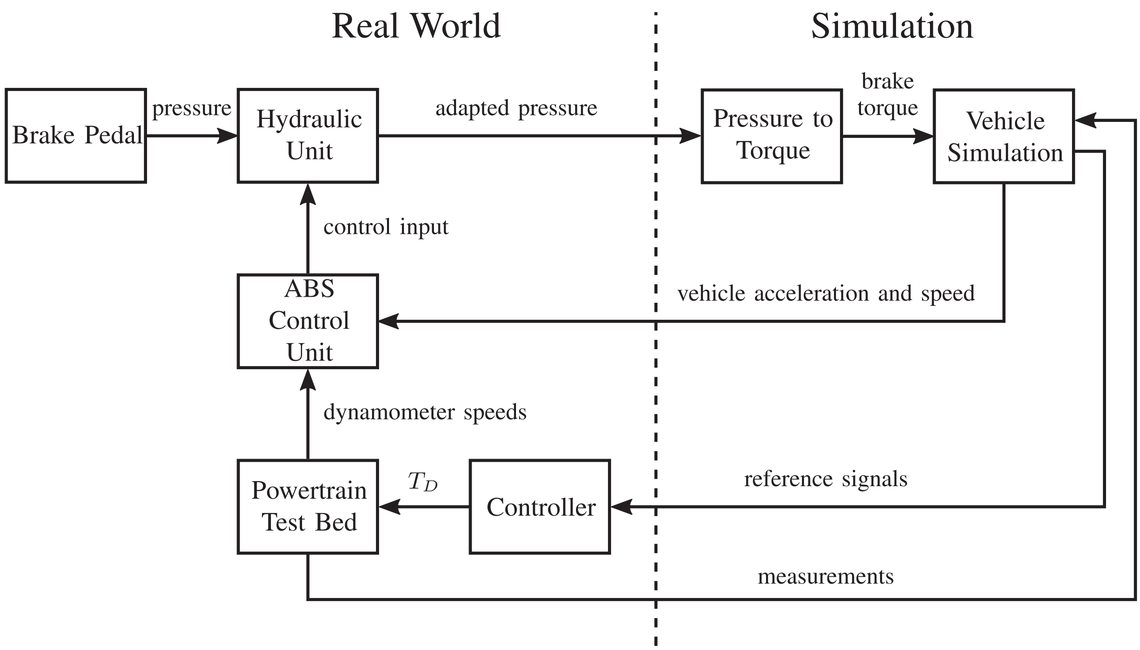

FIGURE 20. **Block diagram of the ABS testing procedure in PHIL configuration. The vehicle, its brakes, and its ABS control unit exist in reality, while the tires and the chassis are simulated.**

Fig. 19 focuses on the torque control with feedforward control. Here, the solid line in the upper diagram again depicts the reference, which is the expected torque $T_{\mathrm{Shaft}}^{\mathrm{ref}}$; see (23). The dash-dotted line represents the measured shaft torque at the test bed. Again, the measurements of the rear left side are visualized. Analogous to the previous figure, the lower plot represents the input signal. As can be seen, the desired shaft torque is tracked well. The feedback controller only needs to perform minor corrections similar to the previously shown concept.

Generally, the results in this section prove that all three investigated control concepts lead to satisfying outcomes at powertrain test beds in PHIL configuration. Particularly, for this highly sophisticated test bed setup, a free choice of the control concepts can be made, and all of the controllers can be implemented easily with minimum tuning effort. However, in the case of known shortcomings at the test bed, an appropriate control concept can be chosen according to the simulation results from the previous section; see Table 1.

3) FULL-BRAKING WITH ABS

The last maneuver which is presented is full-braking with ABS. Generally, the underlying goal of an ABS is to improve the traction and the handling of a vehicle. If ABS testing on a powertrain test bed in PHIL configuration is feasible, and consequently other vehicle dynamic control systems, several advantages result, such as identical environmental conditions while testing. Moreover, time and costs can be saved by conducting the experiments on test beds, and automated testing is enabled.

This maneuver is demanding for the controllers as the torques and speeds rapidly change, and thus, it is well suited for verifying if the control concepts can cope with highly dynamic tests.

In Fig. 20, a block diagram shows the signal flow in this experiment. First, the vehicle slowly accelerates to 45 km/h in simulation on a surface with a road coefficient μ of only 0.08, which is about 10% of the usual value on a dry road. Then, the brake pedal at the test bed is fully actuated via a linear motor. Depending on the vehicle speed, vehicle acceleration, and the dynamometer speeds, the ABS control unit adjusts the pressures of all four brakes via a hydraulic unit. Since the chassis is not moving at the test bed, the vehicle speed and acceleration from the simulation is utilized, while the actual ABS control unit is used. The brake calipers are detached from the vehicle, and metal pieces are clamped between them as they would overheat without the cooling airflow of a real drive. The resulting brake pressures are then passed on to the simulation, where they are processed into brake torques. Apart from the brake torques, the PHIL setup is identical to the previous tests; see Fig. 3. Remarkably, the ABS control loop leads through the real world and the simulation; see Fig. 20, which requires fast control actions and makes this maneuver particularly challenging.

The vehicle speed and the brake pressure during the maneuver are shown in Fig. 21. After the speed of 45 km/h is reached, the brake is actuated, and the ABS immediately intervenes by adjusting the brake pressures.

In Fig. 22, a comparison of all control concepts of this maneuver on the rear left side of the powertrain is shown. The upper plot shows the wheel speeds ω_W, and the lower

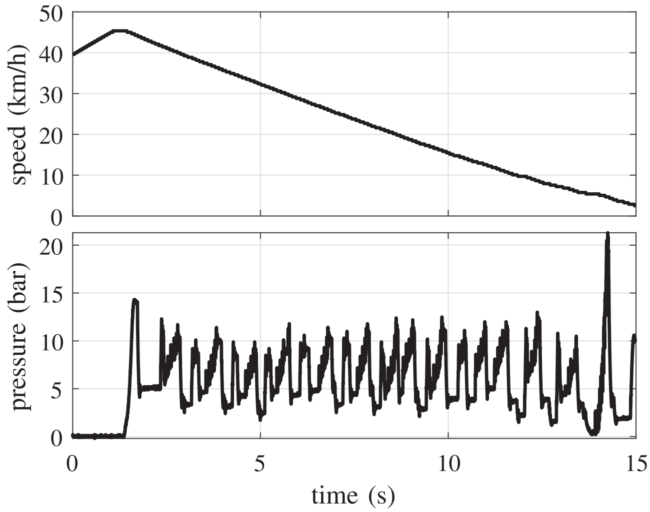

FIGURE 21. Vehicle speed and brake pressure of the rear left side during braking. The ABS control unit constantly adapts the pressure to reduce wheel slip and improve traction.

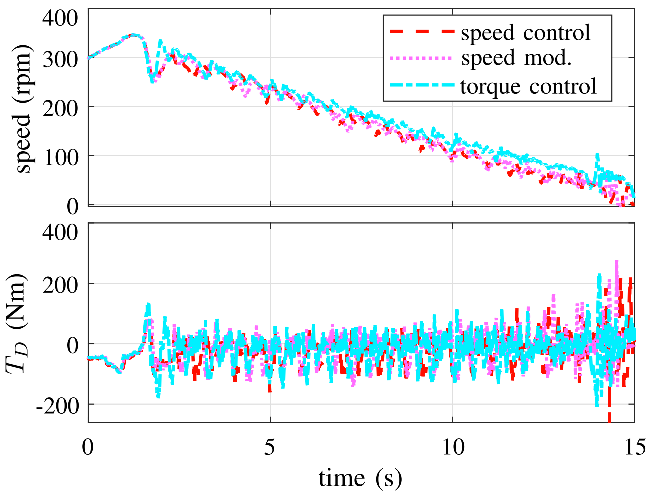

FIGURE 22. Comparison of the different approaches in a full-braking scenario with ABS.

diagram depicts the dynamometer torques T_D from the rear left side of the test bed. As can be seen, the speeds rapidly change up and down because the ABS tries to limit the wheel slip. The changing brake pressures at the test bed influence the braking torque in the simulation, causing these fast changes in speed. Except, in the beginning, the fluctuations in the speed are different, which is caused by random events as there are real sensors involved in this run. The important thing here is that their shape is the same, which is clearly the case. It is also noted that the ABS, which itself was not part of the investigations, performs well since it can slow down the vehicle without locking up the wheels.

The full-braking maneuver with ABS is one of the most dynamic maneuvers in powertrain PHIL testing. With its numerous incorporated sensors and even built-in ABS, it could be proved that all three control concepts are effective and suitable for this task. It can be assumed that other vehicle dynamics controls can also be tested through this setup.

V. CONCLUSION

In this article, different control strategies for entire powertrain test beds in PHIL configuration were first explained and then, compared in simulation and on a modern powertrain test bed. One of the control strategies, which, in contrast to other methods, accepts torque instead of speed signals as references, is extended to match the performance of the other concepts. Particularly, this control concept is beneficial in the case of imprecise dynamometer torques, where it can quickly correct deviations from the requested torques. On the other hand, it is more prone to time delays in communication between the test bed and vehicle simulation. The outcomes were also summarized in a table showing each method's advantages and disadvantages, suggesting what method should be employed in the presence of certain deficits at powertrain test beds.

The implementation on a state-of-the-art powertrain test bed proved the technical feasibility of all control concepts in practice. On highly dynamic maneuvers, it was demonstrated that completely different control approaches led to results that corresponded well with real driving tests. Even actual vehicle dynamic control systems could be tested, which relied on real and simulated signals.

In the future, connected test beds will certainly be an essential topic in the automotive industry. They enable PHIL testing with locally distributed test beds and simulation environments, leading to even more time savings and a further decrease in costs. Through the larger spatial distances, time delays in the signal flow become more dominant, forcing the attention to time delay compensation techniques.

ACKNOWLEDGMENT

The authors acknowledge the TU Wien Bibliothek for financial support through its Open Access Funding Program.

REFERENCES

[1] M. Bacic, "On hardware-in-the-loop simulation," in *Proc. IEEE 44th Conf. Decis. Control*, 2005, pp. 3194–3198, doi: 10.1109/CDC.2005.1582653.
[2] S. Lentijo, S. D'Arco, and A. Monti, "Comparing the dynamic performances of power hardware-in-the-loop interfaces," *IEEE Trans. Ind. Electron.*, vol. 57, no. 4, pp. 1195–1207, Apr. 2010, doi: 10.1109/TIE.2009.2027246.
[3] N. Stegmaier, *Regelung Von Antriebsstrangprüfständen*. New York, NY, USA: Springer, 2019.
[4] O. Gietelink, J. Ploeg, B. De Schutter, and M. Verhaegen, "Development of advanced driver assistance systems with vehicle hardware-in-the-loop simulations," *Veh. Syst. Dyn.*, vol. 44, no. 7, pp. 569–590, 2006, doi: 10.1080/00423110600563338.
[5] O. Gietelink, J. Ploeg, B. De Schutter, and M. Verhaegen, "Development of a driver information and warning system with vehicle hardware-in-the-loop simulations," *Mechatronics*, vol. 19, no. 7, pp. 1091–1104, 2009, doi: 10.1016/j.mechatronics.2009.04.012.
[6] R. Isermann, J. Schaffnit, and S. Sinsel, "Hardware-in-the-loop simulation for the design and testing of engine-control systems," *Proc. 5th IFAC Workshop Algorithms Architecture Real Time Control*, vol. 31, no. 4, pp. 1–10, 1998, doi: 10.1016/S1474-6670(17)42125-2.

[7] R. Isermann, J. Schaffnit, and S. Sinsel, "Hardware-in-the-loop simulation for the design and testing of engine-control systems," *Control Eng. Pract.*, vol. 7, no. 5, pp. 643–653, 1999, doi: 10.1016/S0967-0661(98)00205-6.

[8] A. Mayyas, R. Prucka, P. Pisu, and I. Haque, "Chassis dynamometer as a development platform for vehicle hardware in-the-loop "VHiL"," *SAE Int. J. Commercial Veh.*, vol. 6, no. 2013-01-9018, pp. 257–267, 2013, doi: 10.4271/2013-01-9018.

[9] AVL VSM, "AVL VSM vehicle simulation," Accessed on: Jul. 25, 2022. [Online]. Available: https://www.avl.com/-/avl-vsm-vehicle-simulation

[10] R. S. Benson and R. Pick, "Recent advances in internal combustion engine instrumentation with particular reference to high-speed data acquisition and automated test bed," in *Proc. SAE Int. Off-Highway Powerplant Congr. Expo.*, 1974, doi: 10.4271/740695.

[11] M. Forstinger, R. Bauer, A. Hofer, and W. Rossegger, "Multivariable control of a test bed for differential gears," *Control Eng. Pract.*, vol. 57, pp. 18–28, 2016, doi: 10.1016/j.conengprac.2016.08.010.

[12] J. Andert, S. Klein, R. Savelsberg, S. Pischinger, and K. Hameyer, "Virtual shaft: Synchronized motion control for real time testing of automotive powertrains," *Control Eng. Pract.*, vol. 56, pp. 101–110, 2016, doi: 10.1016/j.conengprac.2016.08.005.

[13] C. Schyr, S. Jakubek, and G. Stempfer, "A new method of coupling HiL-simulation and engine testing based on AUTOSAR-compliant control units," in *Proc. SAE World Congr. Exhib.*, 2009, doi: 10.4271/2009-01-1521.

[14] S. Jiang, M. H. Smith, J. Kitchen, and A. Ogawa, "Development of an engine-in-the-loop vehicle simulation system in engine dynamometer test cell," in *Proc. SAE World Congr. Exhib.*, 2009, doi: 10.4271/2009-01-1039.

[15] B. Yang, L. Guo, and J. Ye, "Real-time simulation of electric vehicle powertrain: Hardware-in-the-loop (hil) testbed for cyber-physical security," in *Proc. IEEE Transp. Electrific. Conf. Expo.*, 2020, pp. 63–68, doi: 10.1109/ITEC48692.2020.9161525.

[16] S. Brennan, A. Alleyne, and M. DePoorter, "The illinois roadway simulator—A hardware-in-the-loop testbed for vehicle dynamics and control," in *Proc. IEEE Amer. Control Conf.*, 1998, vol. 1, pp. 493–497, doi: 10.1109/ACC.1998.694716.

[17] H.-J. Von Thun, "Test for testing the driveline of a vehicle," Germany Patent DE3812824A1, 1989. [Online]. Available: https://patents.google.com/patent/DE3812824A1

[18] M. Pfeiffer, "Test stand for checking performance of power transmission of motor vehicle, has drive supporting system reproduced with impact on brake of wheel, where braking torque is determined by brake demand of drive supporting system," Germany Patent DE102006035502B3, 2008. [Online]. Available: https://patents.google.com/patent/DE102006035502B3

[19] S. Germann, "Method for simulating the behavior of a vehicle on a road," Germany Patent DE19910967C1, 2000. [Online]. Available: https://patents.google.com/patent/DE19910967C1

[20] N. Geiss, "Method and device for testing a four-wheel drive unit" Germany Patent DE3801647C2, 1995. [Online]. Available: https://patents.google.com/patent/DE3801647C2

[21] J. Kronawitter, "Method for operating a test stand for vehicle power transmissions," European Patent Office Patent EP2161560A2, 2008. [Online]. Available: https://patents.google.com/patent/EP2161560A2

[22] R. Bauer, "New methodology for dynamic drive train testing," SAE Technical Paper, Tech. Rep., 2011.

[23] S. C. Oh, "Evaluation of motor characteristics for hybrid electric vehicles using the hardware-in-the-loop concept," *IEEE Trans. Veh. Technol.*, vol. 54, no. 3, pp. 817–824, May 2005, doi: 10.1109/TVT.2005.847228.

[24] R. Bauer, "Neues Regelkonzept für die dynamische Antriebsstrangprüfung," in *Steirisches Seminar über Regelungstechnik und Prozessautomatisierung*. Citeseer, vol. 17, 2011, p. 104.

[25] V. Ivanov et al., "Connected and shared X-in-the-loop technologies for electric vehicle design," *World Elec. Veh. J.*, vol. 10, no. 4, 2019, Art. no. 83, doi: 10.3390/wevj10040083.

[26] V. Schreiber, K. Augsburg, V. Ivanov, and H. Fujimoto, "Novel developing environment for automated and electrified vehicles using remote and distributed X-in-the-loop technique," in *Proc. IEEE Veh. Power Propulsion Conf.*, 2020, pp. 1–5, doi: 10.1109/VPPC49601.2020.9330996.

[27] S. Guo, Y. Liu, Y. Zheng, and T. Ersal, "A delay compensation framework for connected testbeds," *IEEE Trans. Syst., Man, Cybern. Syst.*, vol. 52, no. 7, pp. 4163–4176, Jul. 2022, doi: 10.1109/TSMC.2021.3091974.

[28] V. Schreiber and V. Ivanov, "Optimization using a shared and distributed X-in-the-loop testing environment," in *Proc. IEEE Veh. Power Propulsion Conf.*, 2021, pp. 1–6, doi: 10.1109/VPPC53923.2021.9699231.

[29] M. Mitschke and H. Wallentowitz, *Dynamik Der Kraftfahrzeuge*. Berlin, Germany: Springer, 1972.

[30] R. Gabriel, W. Leonhard, and C. J. Nordby, "Field-oriented control of a standard ac motor using microprocessors," *IEEE Trans. Ind. Appl.*, vol. IA-16, no. 2, pp. 186–192, Mar. 1980, doi: 10.1109/TIA.1980.4503770.

[31] W. Li, M. Yin, Z. Chen, and Y. Zou, "Inertia compensation scheme for wind turbine simulator based on deviation mitigation," *J. Modern Power Syst. Clean Energy*, vol. 5, no. 2, pp. 228–238, 2017, doi: 10.1007/s40565-016-0202-y.

[32] J. Puranen et al., "Induction motor versus permanent magnet synchronous motor in motion control applications: A comparative study," Ph.D. dissertation, Lappeenranta Univ. Technology, 2006.

[33] L. Ljung, *System Identification: Theory for the User*, Prentice Hall PTR, 1999.

[34] L. Ljung, *System Identification Toolbox: User's Guide*. Citeseer, 1995.